Knowledge-based Planning using Pseudo-structures for Volumetric Modulated arc Therapy (VMAT) of Postoperative Uterine Cervical Cancer: A Multi-Institutional Study

Tatsuya Kamima
Cancer Institute Hospital, Japanese Foundation for Cancer Research
Yoshihiro Ueda
Osaka International Cancer Institute: Osaka Kokusai Gan Center
Jun-ichi Fukunaga
Kyushu University Hospital: Kyushu Daigaku Byoin
Mikoto Tamura
Kindai University
Yumiko Shimizu
Seirei Hamamatsu Hospital: Seirei Hamamatsu Byoin
Yuta Muraki
Seirei Hamamatsu Hospital: Seirei Hamamatsu Byoin
Yasuo Yoshioka
Cancer Institute Hospital, Japanese Foundation for Cancer Research
Nozomi Kitamura
Cancer Institute Hospital, Japanese Foundation for Cancer Research
Yuya Nitta
Osaka International Cancer Institute: Osaka Kokusai Gan Center
Masakazu Otsuka
Kindai University: Kinki Daigaku
Hajime Monzen (hmon@med.kindai.ac.jp)
Graduate School of Medical Sciences, Kindai University

Research

Keywords: Knowledge-based planning, RapidPlan, Cervical cancer, Pseudo-structure

Posted Date: November 24th, 2020

DOI: https://doi.org/10.21203/rs.3.rs-113049/v1

Version of Record: A version of this preprint was published at Reports of Practical Oncology and Radiotherapy on August 12th, 2021. See the published version at https://doi.org/10.5603/RPOR.a2021.0089.

Abstract

Background: The aim of this study was to investigate the performance of the RapidPlan knowledge-based treatment planning system using models including registered pseudo-structures, and to determine how many structures are required for automatic optimization of volumetric modulated arc therapy (VMAT) for postoperative uterine cervical cancer.

Methods: Pseudo-structures were retrospectively contoured for patients who had completed treatment at one of five institutions. For 22 patients, RPs were generated with a single optimization for models with two (RP_2), four (RP_4), or five (RP_5) registered structures, and the dosimetric parameters of these models were compared with a clinical plan with several optimizations. The total times for pseudo-structure creation and optimization were also measured.

Results: Most dosimetric parameters showed no major differences between each RP. In particular, the rectum D_{max}, V_{50Gy}, and V_{40Gy} with RP_2, RP_4, and RP_5 were not significantly different, and were lower than those of the clinical plan. In addition, the average proportions of plans achieving acceptable criteria for all dosimetric parameters were 98%, 99%, 98%, and 98% for the clinical plan, RP_2, RP_4, and RP_5, respectively. The average times for the creation and optimization of pseudo-structures were 105, 17, 21, and 29 minutes, for the clinical plan, RP_2, RP_4, and RP_5, respectively.

Conclusions: The RapidPlan model with two registered pseudo-structures could generate clinically acceptable plans while saving time. This modeling approach using pseudo-structures could possibility be used for the VMAT planning process.

Background

Volumetric modulated arc therapy (VMAT) with concurrent chemotherapy has been widely used for post-operative patients with uterine cervical cancer [1]. VMAT can achieve excellent treatment outcomes for cervical cancer while effectively reducing gastrointestinal and urinary toxicity in comparison with three-dimensional conformal radiotherapy [2].

Recently, there has been interest in adaptive radiotherapy (ART) for the pelvic region, in which the radiation treatment plan delivered to a patient is modified during the radiotherapy course to account for temporal changes in anatomy due to weight loss, internal motion, and tumor shrinkage [3]. In the treatment of cervical cancer in particular, large and complex geometrical day-to-day variations in the pelvic region of the bladder, rectum, and bowel can limit the potential positive effects of VMAT [4]. Therefore, online ART may be the most effective strategy for accurate irradiation when faced with daily tumor and normal tissue variations, although the replanning process including re-contouring and re-optimization needs to be completed within a short period of time [5].

The RapidPlan treatment planning system (RP; Varian Medical Systems, Palo Alto CA, USA), which performs knowledge-based planning (KBP), can improve both plan consistency and planning efficiency

[6]. The RP model is made using structures representing the target volumes and organs at risk (OARs), the dose prescription, and the beam arrangements of previous clinical plans. Many studies have reported that KBP can reduce inter-institutional variations in plan quality, reduce treatment planning times using single optimization, and improve dose sparing of OARs compared with clinical manually-optimized plans [7–13]. The mechanical performance and dosimetric accuracy of RP have also been verified, showing that RP can be safely used in clinical practice [14]. Moreover, it was reported that adaptive plans could be generated with the assistance of RP [15, 16], and a previous study reported that the performance of RP was influenced by the plan quality registered in the model [17, 18]. However, the original target volumes and OAR structures were registered in most of the RP models used in these studies, and the contouring process part of the treatment planning still remains labor-intensive and time-consuming.

In practice, the planner generates the contours of virtual structures, the so-called “pseudo-structures”, to which the planning dose constraints are imposed [19]. These pseudo-structures can be created very simply and easily using Boolean operations. Castriconi et al. showed the efficiency of plan creation by combining RP and pseudo-structure methods, but did not register the pseudo-structure in the model [20]. Therefore, there has been no report evaluating the performance of RP using pseudo-structures registered in the model. Moreover, the impact of the number of registered structures in the model on the performance of RP also remains unclear.

In this study, we retrospectively contoured simple pseudo-structures in cervical cancer patients who were previously treated at one of the involved institutes. Three patterns of models with different numbers of registered structures were created at each institute, and these models were used to generate treatment plans for new patients not used in the models. The aim of this study was to investigate the performance of RP using a model with registered pseudo-structures, and to determine how many structures are required for automatic optimization of VMAT for postoperative uterine cervical cancer.

Methods

Clinical VMAT plan setting for cervical cancer at each institute registered in the model

This study enrolled five Japanese institutes (A–E). These institutes used VMAT to treat patients with high-risk postoperative uterine cervical cancer. The clinical VMAT plans at each institute were created mainly according to the Japan Clinical Oncology Group (JCOG) 1402 protocol [21, 22]. The clinical target volumes (CTVs) and OARs in the JCOG1402 protocol were contoured according to the CTV contouring guidelines [23, 24] and the Radiation Therapy Oncology Group guidelines for OARs [25]. At each institute, these clinical VMAT plans were created with manual optimization using an unlimited number of pseudo-structures.

Common pseudo-structure contours

We propose the use of pseudo-structures as a more efficient method for the VMAT optimization and contouring process. These pseudo-structures around the planning target volume (PTV) were introduced with the aim of managing the dose gradient around the PTV. For patients who had completed treatment at one of the institutions, three common pseudo-structures were retrospectively contoured, according to the procedure manual:

1) Control_ Anterior (A): Control_A was created from the union of the bowel bag and bladder area, and was cropped from the PTV by 7 mm.

2) Control_ Peripheral (P): Control_P was created with an expansion from the PTV of 2–3 cm and cropping from the PTV and Control_A by 7 mm.

3) Control_ A P: Control_ A P was created from the union of Control_A and Control_P.

These pseudo-structures were inspired by those used in clinical practice. Details of the contoured pseudo-structures and femoral heads are shown in Fig. 1. These pseudo-structures were simply created using Boolean operations and interpolation.

RapidPlan model configuration

The RP algorithm was explained in detail by Fogliata et al. [16]. First, in the model building, the contoured pseudo-structures of the patients were registered. To evaluate the impact of the number of structures registered in the model on the performance of RP, three model patterns with different numbers of registered structures were created at each institute. The process for contouring pseudo-structures and configuring the three model patterns is shown in Fig. 2. Model_2, Model_4, and Model_5 had two, four, and five structures registered in the model, respectively. The number of registered cases of each model type at institutes A, B, C, D, and E were 29, 20, 26, 70, and 30, respectively. Details of the RP models of each institute are shown in Table 1.

Table 1
The RapidPlan model data at each institution.

Model					
	A	B	C	D	E
	Mean volume ± SD [cm^3] Mean dose ± SD [%]				
PTV	1105.9 ± 99.7 100.5 ± 0.4	1009.6 ± 166.3 103.2 ± 1.3	973.1 ± 138.0 99.2 ± 0.2	983.6 ± 130.8 98.9 ± 0.2	912.1 ± 149.6 99.2 ± 0.1
Control_A	864.4 ± 237.2 53.1 ± 3.0	1162.2 ± 502.9 42.5 ± 5.3	1299.1 ± 365.1 45.0 ± 4.6	1434.5 ± 441.1 41.8 ± 4.7	1185.8 ± 419.1 43.9 ± 2.9
Control_P	2973.7 ± 631.5 45.9 ± 4.2	4217.5 ± 1258.9 43.0 ± 3.6	2792.0 ± 465.2 47.7 ± 2.5	3235.6 ± 553.2 41.3 ± 3.2	2683.4 ± 344.1 50.8 ± 2.6
Control_AP	3967.5 ± 480.5 46.6 ± 4.1	5380.2 ± 1708.7 42.9 ± 3.6	4099.0 ± 626.3 46.7 ± 2.4	4696.8 ± 769.8 41.2 ± 3.1	3869.8 ± 527.4 48.7 ± 2.3
Femoral head_R	38.1 ± 5.5 50.5 ± 3.8	44.0 ± 9.1 54.1 ± 10.8	48.8 ± 18.7 44.2 ± 9.9	36.8 ± 5.8 45.4 ± 7.1	43.0 ± 11.1 47.6 ± 4.0
Femoral head_L	37.8 ± 5.0 51.8 ± 3.7	44.7 ± 9.9 53.8 ± 10.7	48.2 ± 17.5 48.2 ± 10.1	36.6 ± 5.7 45.0 ± 6.1	42.2 ± 10.9 48.1 ± 3.5

Abbreviations: PTV: planning target volume, Control_A: Control_ Anterior, Control_P: Control_ Peripheral, Femoral head_R: right femoral head, Femoral head_L: left femoral head

The second step was a training phase based on information extracted from data such as dosimetric and geometric information. These data could be analyzed from the website of Model Analytics (https://ModelAnalytics.varian.com). The Model Analytics data also included information about structures or patients that were found to be potential outliers according to numerical metrics, although we did not remove these statistical outliers from the training set used in this study.

The third step was selection of the optimization objectives and their priorities. Line, upper, and lower objectives, and priorities, were selected at each institute for each structure in the model, as shown in Table 2. Finally, these models were delivered to institute A to create treatment plans for common patients. Written informed consent was obtained from all patients, and the institutional ethics committee approved this study (Japanese Foundation for Cancer Research review board number: 2019 – 1045).

Table 2
Configuration of the Objective for each structure used in RapidPlan.

Structures	Institute	Objective	Vol. [%]	Dose	Priority
PTV	A	Upper	0	52.4 Gy	70
		Upper	0.3	52.0 Gy	70
		Lower	100	50.4 Gy	70
		Lower	95	51.4 Gy	70
	B	Upper	0	101%	Generated
		Lower	100	99%	Generated
	C	Upper	0	100%	Generated
		Lower	100	100%	Generated
	D	Upper	0	100%	Generated
		Lower	100	100%	Generated
	E	Upper	0	101%	100
		Lower	100	100%	120
Control_A	A	Upper	0	35.0 Gy	Generated
		Upper	Generated	30.0 Gy	Generated
		Line	Generated	Generated	Generated
	B	Line	Generated	Generated	Generated
		Line	Generated	Generated	Generated
	D	Line	Generated	Generated	Generated
.	E	Line	Generated	Generated	Generated
Control_P	A	Upper	Generated	35.0 Gy	Generated
		Line	Generated	Generated	Generated
	B	Line	Generated	Generated	Generated
	C	Upper	0	100%	Generated
		Line	Generated	Generated	Generated
	D	Line	Generated	Generated	Generated

Abbreviations: PTV: planning target volume, Control_A: Control_ Anterior, Control_P: Control_ Peripheral, Femoral head_R: right femoral head, Femoral head_L: left femoral head

Structures	Institute	Objective	Vol. [%]	Dose	Priority
	E	Line	Generated	Generated	Generated
Control_A P	A	Upper	0	35.0 Gy	Generated
		Upper	Generated	30.0 Gy	Generated
		Line	Generated	Generated	Generated
	B	Line	Generated	Generated	Generated
	C	Upper	0	100%	Generated
		Line	Generated	Generated	Generated
	D	Line	Generated	Generated	Generated
	E	Upper	0	45.0 Gy	150
		Upper	50	25.0 Gy	Generated
		Line	Generated	Generated	Generated
Femoral head_R	A	Upper	Generated	30.0 Gy	Generated
		Line	Generated	Generated	Generated
	B	Line	Generated	Generated	Generated
	C	Line	Generated	Generated	Generated
	D	Line	Generated	Generated	Generated
	E	Line	Generated	Generated	Generated
Femoral head_L	A	Upper	Generated	30.0 Gy	Generated
		Line	Generated	Generated	Generated
	B	Line	Generated	Generated	Generated
	C	Line	Generated	Generated	Generated
	D	Line	Generated	Generated	Generated
	E	Line	Generated	Generated	Generated

Abbreviations: PTV: planning target volume, Control_A: Control_ Anterior, Control_P: Control_ Peripheral, Femoral head_R: right femoral head, Femoral head_L: left femoral head

Evaluation of RapidPlan performance

The RP performance evaluation dataset consisted of the CT data and clinical manually-optimized plans of 22 postoperative uterine cervical cancer patients treated between 2015 and 2019 at institute A. This dataset was independent of that used in the model library. For each patient, a CT-scan was acquired with

2.0-mm slice thickness and a 50-cm field of view. Pseudo-structures were also retrospectively contoured on the CT images.

Without manual intervention and normal tissue objectives, VMAT plans were created at institute A with a single optimization using each RP model and the setting optimization objectives of each institute. For the two-arc VMAT, plans with 10-MV photon beams were created using the Photon Optimizer and Anisotropic Analytic Algorithm in the Eclipse treatment planning system Ver 15.6 (Varian Medical Systems, Palo Alto, CA, USA). A dose covering 50% of the PTV of 50.4 Gy in 28 fractions was applied to both the nodal and vaginal cuff PTVs [22]. The plans created by Model_2, Model_4, and Model_5 were identified as RP_2, RP_4, and RP_5, respectively. Comparisons of the treatment plans created by each model were performed using the JCOG1402 dose constraints for PTV and OARs to evaluate the number of structures required for the RP. For the PTV, $D_{98\%}$, $D_{95\%}$, and $D_{2\%}$ were used, whereas D_{max} was used for the overlap between the PTV and bowel bag. For OARs, we used the D_{max}, V_{50Gy}, and V_{40Gy} of rectum, D_{max} and V_{45Gy} of bladder, V_{40Gy} of bowel bag, V_{40Gy} and V_{10Gy} of pelvic bones, V_{30Gy} of each femoral head, and D_{max} of the body. Figure 3 shows the process for model transfer and plan comparison.

To evaluate the target coverage, we analyzed the homogeneity index (HI) and conformity index (CI) for the PTV. The HI was calculated as [26–28]:

$$HI = \frac{D_{2\%} - D_{98\%}}{D_p} \qquad (1)$$

Where $D_{2\%}$= minimum dose to 2% of the target volume indicating the “maximum dose”, $D_{98\%}$= minimum dose to 98% of the target volume, indicating the “minimum dose”, and D_p = prescribed dose. The ideal value is zero, and increases as homogeneity decreases.

CI was calculated as follows [29],

$$CI = \frac{V_{RI}}{TV} \qquad (2)$$

Where V_{RI} is the volume of the reference dose and TV is the target volume. The ideal value is 1.

Planning efficiency

The average planning times of the clinical manually-optimized plans registered in the model (target contouring, OAR contouring, pseudo-structure creation, and optimization times) were recorded at each

institute. In the same way, the average planning times (pseudo-structure creation and optimization time) of the RP plans were also recorded.

Statistical analysis

Statistical analyses were performed to identify differences in the plans created by each model. The Kruskal-Wallis test was used to compare the three model patterns. When the Kruskal-Wallis test indicated a statistically significant difference, the Steel-Dwass test was used to determine which pair-wise comparisons differed. All statistical analyses were conducted with JMP 15.1.0 (SAS Institute, Cary, NC, USA). A value of $p < 0.05$ was considered statistically significant.

Results

Inter-model comparisons

A summary of the dosimetric parameters is listed in Table 3. Box-and-whisker plots of rectum, bowel bag, and femoral head doses for each RP plan at each institute are shown in Fig. 4. Most dosimetric parameters showed no major differences across the models, except for the femoral head. The rectum in particular showed no significant differences between the plans created using the respective models at all institutions for all dosimetric parameters. Additionally, the rectum dose of the RP plans was lower than that of the clinical plan.

Table 3
Summary of the dosimetric parameters.

Structures	Average ± SD [%]	Clinical plan	RP_2	RP _4	RP_5	P value
PTV	$D_{98\%}$	93.3 ± 1.0	94.5 ± 1.8	94.9 ± 1.5	94.5 ± 1.2	0.03
	$D_{95\%}$	95.1 ± 0.8	95.8 ± 1.5	96.2 ± 1.3	96.0 ± 1.0	0.1
	$D_{2\%}$	103.0 ± 0.4	102.7 ± 0.5	102.6 ± 0.4	102.8 ± 0.4	< 0.001
Overlap between PTV and bowel bag	D_{max}	104.5 ± 0.6	105.0 ± 1.0	105.1 ± 1.0	105.4 ± 1.0	< 0.01
Rectum	V_{40Gy}	82.9 ± 13.4	77.9 ± 15.3	80.5 ± 14.9	82.3 ± 15.7	0.06
	V_{50Gy}	33.7 ± 15.9	23.4 ± 10.9	25.4 ± 10.6	25.4 ± 11.3	0.27
	D_{max}	103.8 ± 0.7	102.6 ± 0.9	102.7 ± 1.1	103.0 ± 1.7	0.63
Bladder	V_{45Gy}	34.2 ± 8.3	39.0 ± 10.2	43.2 ± 12.9	36.9 ± 9.5	< 0.001
	D_{max}	103.9 ± 0.8	103.7 ± 1.0	103.7 ± 1.0	104.1 ± 1.1	< 0.001
Bowel bag	V_{40Gy}	32.5 ± 6.6	34.5 ± 8.7	35.8 ± 9.1	31.6 ± 7.5	< 0.01
Pelvic bones	V_{10Gy}	87.3 ± 3.0	87.8 ± 3.2	86.8 ± 3.5	86.9 ± 3.3	0.01
	V_{40Gy}	20.6 ± 3.8	18.5 ± 3.5	18.7 ± 3.3	20.5 ± 4.2	< 0.001
Femoral head_R	V_{30Gy}	18.9 ± 6.4	17.5 ± 11.9	7.4 ± 8.0	8.0 ± 8.9	< 0.001
Femoral head_L	V_{30Gy}	17.3 ± 7.8	16.2 ± 14.8	6.9 ± 6.9	9.2 ± 7.4	< 0.001
Body	D_{max}	106.6 ± 1.1	105.9 ± 1.0	105.9 ± 1.1	106.2 ± 1.2	0.21

Abbreviations: PTV: planning target volume, Femoral head_R: right femoral head, Femoral head_L: left femoral head, D_{max}: maximum dose, $D_{98\%}$, $D_{95\%}$ and $D_{2\%}$ the dose received by at least 98%, 95% and 2.0% of the volume, V_{50Gy}, V_{45Gy}, V_{40Gy}, V_{30Gy} and V_{10Gy} the OAR volume that receives a dose exceeding 50 Gy, 45 Gy, 40 Gy, 30 Gy and 10 Gy.

For the femoral head, there were statistically significant differences between RP_2, RP_4, and RP_5 at all institutes except institute B. Dose sparing of the femoral heads was worse with RP_2 than with RP_4 and RP_5, but better than that of the clinical plan.

Table 4 shows the proportions of clinical and RP plans achieving the acceptable criteria of the JCOG 1402 protocol. Close to 100% of each of the RP plans achieved the acceptable criteria for most dosimetric parameters. A dose reduction to the femoral head was not achieved with RP_2 in comparison with other models, although performance in terms of the achievement rate was high. For the rectum, although only 74–85% of the RP plans achieved acceptable V_{40Gy} criteria, the clinical plans achieved similar results.

Table 4
The proportions of plans achieving acceptable criteria of the JCOG 1402 protocol.

Structures		Acceptable objective	Clinical plan	RP_2	RP_4	RP_5
PTV	$D_{98\%}$	> 85%	100%	100%	100%	100%
	$D_{95\%}$	> 90%	100%	100%	100%	100%
	$D_{2\%}$	< 115%	100%	100%	100%	100%
Overlap between PTV and bowel bag	D_{max}	< 110%	100%	100%	100%	100%
Rectum	V_{40Gy}	< 95%	77%	85%	79%	74%
	V_{50Gy}	< 60%	95%	100%	100%	100%
	D_{max}	< 120%	100%	100%	100%	100%
Bladder	V_{45Gy}	< 70%	100%	100%	96%	100%
	D_{max}	< 120%	100%	100%	100%	100%
Bowel bag	V_{40Gy}	< 50%	100%	97%	95%	100%
Pelvic bones	V_{10Gy}	< 95%	100%	100%	100%	100%
	V_{40Gy}	< 50%	100%	100%	100%	100%
Femoral head_R	V_{30Gy}	< 60%	100%	100%	100%	99%
Femoral head_L	V_{30Gy}	< 60%	100%	98%	100%	100%
Body	D_{max}	< 120%	100%	100%	100%	100%

Abbreviations: PTV: planning target volume, Femoral head_R: right femoral head, Femoral head_L: left femoral head, D_{max}: maximum dose, $D_{98\%}$, $D_{95\%}$ and $D_{2\%}$ the dose received by at least 98%, 95% and 2.0% of the volume, V_{50Gy}, V_{45Gy}, V_{40Gy}, V_{30Gy} and V_{10Gy} the OAR volume that receives a dose exceeding 50 Gy, 45 Gy, 40 Gy, 30 Gy and 10 Gy.

The PTV HIs (mean ± 1 SD for all institutions) were 0.10 ± 0.01, 0.08 ± 0.02, 0.08 ± 0.02, and 0.08 ± 0.01 for the clinical plan, RP_2, RP_4, and RP_5, respectively. The PTV CIs (mean ± 1 SD for all institutions) were 0.51 ± 0.01, 0.50 ± 0.01, 0.51 ± 0.01, and 0.51 ± 0.02 for the clinical plan, RP_2, RP_4, and RP_5, respectively. Inter-model comparisons of PTV homogeneity and conformity at each institute showed that there were no differences between the models, and that the number of registered structures in the model had no effect on PTV dose. Additionally, at institutes B, C, D, and E, the dose coverage of the PTV was better than that of the clinical plan.

Planning time analysis

Table 5 shows the average planning times of the clinical manually-optimized plan and RP plans, with this time being spent on the various processes of the treatment planning. Using RP_2, RP_4, and RP_5, the average time for the creation of pseudo-structures was reduced by 13 minutes, 9 minutes, and 1 minute, respectively, compared with the clinical plan, while the VMAT planning time was reduced by 88, 84, and 76 minutes, respectively, compared with the clinical plan.

Table 5
Average time spent on various treatment planning processes.

Mean time (minutes)		Clinical plan	RP_2	RP_4	RP_5
Contouring	Targets contouring	105	0	0	0
	OARs contouring	99	0	0	0
VMAT Planning	Pseudo-structures creation	15	2	6	14
	Optimization	90	15	15	15
	Total time of planning	315	17	21	29
Abbreviations: VMAT: volumetric modulated arc therapy, OAR: organs at risk					

Discussion

This multi-institutional study investigated the performance of RP using models with pseudo-structures and determined the optimal number of pseudo-structures for RP models. Inter-model comparisons showed no major differences for most dosimetric parameters, as shown in Table 3 and Fig. 4. Compared with the clinical plans, the RP plans showed better dose coverage and OAR sparing. Furthermore, Table 4 indicates that most RP plans were able to achieve the acceptable criteria of the JCOG 1402 protocol. Previous publications evaluating RP models showed that KBP plans exceeded the clinical accepted plan quality at various anatomical sites [7, 16, 30, 31]. Although the models in these studies were registered with multiple original OAR structures, the RP performance of our models with only 2–5 pseudo-structures registered was found to be similar to that reported in previous publications. Thus, our results show that training RP models with pseudo-structures is a simple and effective approach for creating high quality VMAT plans with RP.

The dosimetric parameter results in Table 3 and Fig. 4, and the proportions of plans achieving acceptable criteria in Table 4, indicate that Model_2 using only the PTV and Control_A P showed good dosimetric performance at all institutes. As shown in Table 2, a line objective was commonly used for Control_A P at each institute. The good dosimetric performance of Model_2 is helped by the use of the line objective defined slightly below the estimated dose volume histogram (DVH) lower bound, which helps to drive the optimization towards the best estimated DVH [32]. As the weights for the points on each line objective are all equal, reducing the average dose for large volume structures may be more effective. However, the dose sparing of the femoral head in RP_2 was the worst among the RP models at each institute. This was

because the Control_A P pseudo-structure did not impose dose constraints locally on the femoral head. However, the proportions of plans achieving acceptable criteria in the right and left femoral heads were 100% and 98%, respectively. Model_5, in which Control_A P was divided and registered in the model, also showed no dose-reduction advantage in the rectum, bladder, and pelvic bone in comparison with Model_2. Therefore, we conclude that the RP model can perform adequately with the registration of two structures.

The potential benefit of this modeling approach using pseudo-structures is time efficiency. In practice, the correcting of tumor and normal tissue variations through modification of the original plan is hampered by the time-consuming re-planning process, which currently represents the major obstacle for large scale implementation of this strategy [33]. Recently, the use of deformable image registration (DIR) for automatic propagation of structures in ART has been widely investigated. However, registration errors may still exist with DIR, especially for structures that are small and lack contrast with the background, and these registration errors could result in significant dosimetric deviation [34]. Additionally, Nelson et al. reported a total planning time of 207.5 minutes for OAR contouring and optimization, even when implementing DIR in an adaptive plan with the assistance of KBP [15]. As Table 5 shows, the plan created using Model_2 took only 17 minutes for the pseudo-structure creation and optimization process. Acharya et al. reported that the median time for online ART using an MR Linac was 26 minutes, including re-contouring, re-optimization, and patient-specific quality assurance [35]. Therefore, this modeling approach using pseudo-structures should be useful for online ART.

The KBP approach has the advantage that its model can be shared by multiple institutions. Sharing of models is considered to be a good method for reducing variability in planning quality across multiple institutions [17]. In the present study, we were able to create a plan achieving acceptable criteria with a model that was created using only a simple procedure manual. Therefore, the model can be easily shared by creating pseudo-structures at each institute. It was also reported that inter-observer contouring variations have a significant impact on dosimetric and radiobiological outcomes in intensity modulated radiation therapy planning [36]. Reducing the number of structures is useful as a means of homogenizing treatment plan quality across institutions.

The planning quality evaluation in this study was conducted only for cervical cancer patients, and there is a limitation in that the methods in this study cannot cover treatment plans for several PTV dose levels using a simultaneous integrated boost (SIB), such as is performed in head and neck cancer patients; management of the dose gradient around PTVs is more complex with SIB-VMAT plans. In addition, the structures used for the dose evaluation were not considered in this study, but may be defined using automatic segmentation methods.

Conclusions

The RP_2 plan achieved clinically-acceptable criteria, and comparable dosimetric parameters to the clinical, RP_4, and RP_5 plans. The RP model with two registered pseudo-structures could generate a

clinically-acceptable plan while saving considerable time. The RP modeling approach was simple and might be useful for online ART.

List Of Abbreviations

ART: Adaptive radiotherapy; CI: conformity index; Control_A: Control_ Anterior; Control_P: Control_ Peripheral; CTV: clinical target volume; DIR: Deformable image registration; D_{max}: Maximum dose; D_p: Prescribed dose; DVH: Dose volume histogram; $D_{X\%}$: Dose received by at least X% of the volume; HI: Homogeneity index; JCOG: Japan clinical oncology group; KBP: Knowledge-based planning; Model_2: Model with two structures registered; Model_4: Model with four structures registered; Model_5: Model with five structures registered; OAR: Organs at risk; PTV: planning target volume; RP: RapidPlan; RP_2: Plans created by Model_2; RP_4: Plans created by Model_4; RP_5: Plans created by Model_5; SIB: simultaneous integrated boost; TV: target volume; VMAT: Volumetric modulated arc therapy; V_{RI}: volume of the reference dose; V_{XGy}: Volume receiving X Gy.

Declarations

Ethics approval and consent to participate:

This study was approved by each institutional ethical review committee with written informed consent provided by the patients.

Consent for publication:

The institutional consent form was obtained from the patients.

Availability of data and material:

The datasets used and/or analyzed during the current study are available from the corresponding author on reasonable request.

Competing interests:

The authors declare that they have no competing interests.

Funding:

We gratefully acknowledge support from the Japanese Society of Radiological Technology (JSRT) Research Grant (2019, 2020). This study was supported by a JSPS KAKENHI Grant [grant number 17

K15817].

Authors' contributions:

Concept and design: TK, YU, JF, MT, YS, YM, MH. Treatment planning: TK, YU, JF, MT, YS, YM, YY, NK, YN, MO, MH. Data analysis: TK, YU, JF, MT, YS, YM, MH. Manuscript preparation: TK, YU, MT, MH. All authors read and approved the final manuscript.

Acknowledgements:

We thank Karl Embleton, PhD, from Edanz Group (https://en-author-services.edanzgroup.com/) for editing a draft of this manuscript.

References

1. Yuan Y, You J, Wang W, Li X. Long-term follow-up of volumetric modulated arc therapy in definitive radiotherapy for cervical cancer: A single-center retrospective experience. Radiation Medicine and Protection, 2020;1:2,81-87.
2. Lin Y, Ouyang Y, Chen K, Lu Z, Liu Y, Cao X. Clinical outcomes of volumetric modulated arc therapy following intracavitary/interstitial brachytherapy in cervical cancer: a single institution retrospective experience. Front Oncol. 2019;9:760.
3. Tan LT, Tanderup K, Kirisits C, de Leeuw A, Nout R, Duke S, et al. Image-guided Adaptive Radiotherapy in Cervical Cancer. Semin Radiat Oncol. 2019;29:284-298.
4. Heijkoop S.T. Plan-of-the-day Adaptive Radiotherapy for Locally Advanced Cervical Cancer. Erasmus University Rotterdam, 2017. http://hdl.handle.net/1765/102419. [accessed 12 July 2020].
5. Liu X, Liang Y, Zhu J, Yu G, Yu Y, Cao Q, et al. A Fast Online Replanning Algorithm Based on Intensity Field Projection for Adaptive Radiotherapy. Front Oncol.2020;10:287.
6. Fusella M, Scaggion A, Pivato N, Rossato MA, Zorz A, Paiusco M. Efficiently train and validate a RapidPlan model through APQM scoring. Med Phys. 2018;45:2611-2619.
7. Tol JP, Delaney AR, Dahele M, Slotman BJ, Verbakel WF. Evaluation of a knowledge-based planning solution for head and neck cancer. Int. J. Radiat. Oncol. Biol. Phys. 2015;91:612-20.
8. Appenzoller LM, Michalski JM, Thorstad WL, Mutic S, Moore KL. Predicting dose-volume histograms for organs-at-risk in imrt planning. Med Phys. 2012;39:7446-61.
9. Krayenbuehl J, Norton I, Studer G, Guckenberger M. Evaluation of an automated knowledge based treatment planning system for head and neck. Radiat Oncol. 2015;10:226.
10. Fogliata A, Nicolini G, Clivio A, Vanetti E, Laksar S, Tozzi A, et al. A broad scope knowledge based model for optimization of VMAT in esophageal cancer: validation and assessment of plan quality among different treatment centers. Radiat Oncol. 2015;10:220.

11. Wu H, Jiang F, Yue H, Li S, Zhang Y. A dosimetric evaluation of knowledge-based VMAT planning with simultaneous integrated boosting for rectal cancer patients. J Appl Clin Med Phys. 2016;17:78-85.
12. Kubo K, Monzen H, Ishii K, Tamura M, Kawamorita R, Sumida I, et al. Dosimetric comparison of RapidPlan and manually optimized plans in volumetric modulated arc therapy for prostate cancer. Phys Med. 2017;44:199-204.
13. Tol JP, Delaney AR, Dahele M, Slotman BJ, Verbakel WF. Evaluation of a knowledge-based planning solution for head and neck cancer. Int J Radiat Oncol Biol Phys. 2015;91:612-20.
14. Tamura M, Monzen H, Matsumoto K, Kubo K, Otsuka M, Inada M, et al. Mechanical performance of a commercial knowledge-based VMAT planning for prostate cancer. Radiat Oncol. 2018;13:163.
15. Fung NTC, Hung WM, Sze CK, Lee MCH, Ng WT. Automatic segmentation for adaptive planning in nasopharyngeal carcinoma IMRT: Time, geometrical, and dosimetric analysis. Med Dosim. 2020;45:60-65.
16. Fogliata A, Wang PM, Belosi F, Clivio A, Nicolini G, Vanetti E, et al. Assessment of a model based optimization engine for volumetric modulated arc therapy for patients with advanced hepatocellular cancer. Radiat Oncol. 2014;9:236.
17. Ueda Y, Fukunaga JI, Kamima T, Adachi Y, Nakamatsu K, Monzen H. Evaluation of multiple institutions' models for knowledge-based planning of volumetric modulated arc therapy (VMAT) for prostate cancer. Radiat Oncol. 2018;13:46.
18. Kamima T, Ueda Y, Fukunaga JI, Shimizu Y, Tamura M, Ishikawa K, et al. Multi-institutional evaluation of knowledge-based planning performance of volumetric modulated arc therapy (VMAT) for head and neck cancer. Phys Med. 2019;64:174-181.
19. Neve W D, Wu Y, Ezzell G. Practical IMRT Planning. Image-guided IMRT. Berlin: Springer; 2006. p. 49-54.
20. Castriconi R, Fiorino C, Passoni P, Broggi S, Di Muzio NG, Cattaneo GM, et al. Knowledge-based automatic optimization of adaptive early-regression-guided VMAT for rectal cancer. Phys Med. 2020;70:58-64.
21. Murakami N, Isohashi F, Hasumi Y, Kasamatu T, Okamoto H, Nakamura K, et al. Single-arm confirmatory trial of postoperative concurrent chemoradiotherapy using intensity modulated radiation therapy for patients with high-risk uterine cervical cancer: Japan Clinical Oncology Group study (JCOG1402). Jpn J Clin Oncol. 2019;49:881-885.
22. Okamoto H, Murakami N, Isohashi F, Kasamatsu T, Hasumi Y, Iijima K, et al. Dummy-run for standardizing plan quality of intensity-modulated radiotherapy for postoperative uterine cervical cancer: Japan Clinical Oncology Group study (JCOG1402). Radiat Oncol. 2019;14:133.
23. Toita T, Ohno T, Kaneyasu Y, Uno T, Yoshimura R, Kodaira T, et al. A consensus-based guideline defining the clinical target volume for pelvic lymph nodes in external beam radiotherapy for uterine cervical cancer. Jpn J Clin Oncol. 2010;40:456-63.

24. Murakami N, Norihisa Y, Isohashi F, Murofushi K, Ariga T, Kato T, et al. Proposed definition of the vaginal cuff and paracolpium clinical target volume in postoperative uterine cervical cancer. Pract Radiat Oncol. 2016;6:5-11.
25. Gay HA, Barthold HJ, O'Meara E, Bosch WR, El Naqa I, Al-Lozi R, et al. Pelvic normal tissue contouring guidelines for radiation therapy: a Radiation Therapy Oncology Group consensus panel atlas. Int J Radiat Oncol Biol Phys. 2012;83:e353-62.
26. Kataria T, Sharma K, Subramani V, Karrthick KP, Bisht SS. Homogeneity Index: An objective tool for assessment of conformal radiation treatments. J Med Phys . 2012;37:207-13.
27. Wu Q, Mohan R, Morris M, Lauve A, Schmidt-Ullrich R. Simultaneous integrated boost intensity-modulated radiotherapy for locally advanced head-and-neck squamous cell carcinomas. I: dosimetric results. Int J Radiat Oncol Biol Phys. 2003;56:573-85.
28. Yoon M, Park SY, Shin D, Lee SB, Pyo HR, Kim DY, et al. A new homogeneity index based on statistical analysis of the dose-volume histogram. J Appl Clin Med Phys. 2007;8:9-17.
29. Feuvret L, Noël G, Mazeron JJ, Beyet P. Conformity Index: a review, Int J Radiat Oncol Biol Phys. 2006; 64:333-342.
30. Hussein M, South CP, Barry MA, Adams EJ, Jordan TJ, Stewart AJ, et al. Clinical validation and benchmarking of knowledge-based IMRT and VMAT treatment planning in pelvic anatomy. Radiother Oncol. 2016;120:473-479.
31. Tinoco M, Waga E, Tran K, Vo H, Baker J, Hunter R, et al. RapidPlan development of VMAT plans for cervical cancer patients in low-and middle-income countries. Med Dosim. 2020;45:172-178.
32. Fogliata A, Cozzi L, Reggiori G, Stravato A, Lobefalo F, Franzese C, et al. RapidPlan knowledge based planning: iterative learning process and model ability to steer planning strategies. Radiat Oncol. 2019;14:187.
33. Cilla S, Ianiro A, Romano C, Deodato F, Macchia G, Buwenge M, et al. Template-based automation of treatment planning in advanced radiotherapy: a comprehensive dosimetric and clinical evaluation. Sci Rep. 2020;10:423.
34. Jishi L, Zhiyuan X, Avinash P, Brian O, Shao H H. Adaptive radiotherapy for nasopharyngeal carcinoma. Ann Nasopharynx Cancer 2020;4:1
35. Acharya S, Fischer-Valuck BW, Kashani R, Parikh P, Yang D, Zhao T, et al. Online Magnetic Resonance Image Guided Adaptive Radiation Therapy: First Clinical Applications. Int J Radiat Oncol Biol Phys. 2016 ;94:394-403.
36. Bhardwaj AK, Kehwar TS, Chakarvarti SK, Sastri GJ. Variations in inter-observer contouring and its impact on dosimetric and radiobiological parameters for intensity-modulated radiotherapy planning in treatment of localised prostate cancer. J Radiother Pract. 2008;7:77-88.

Figures

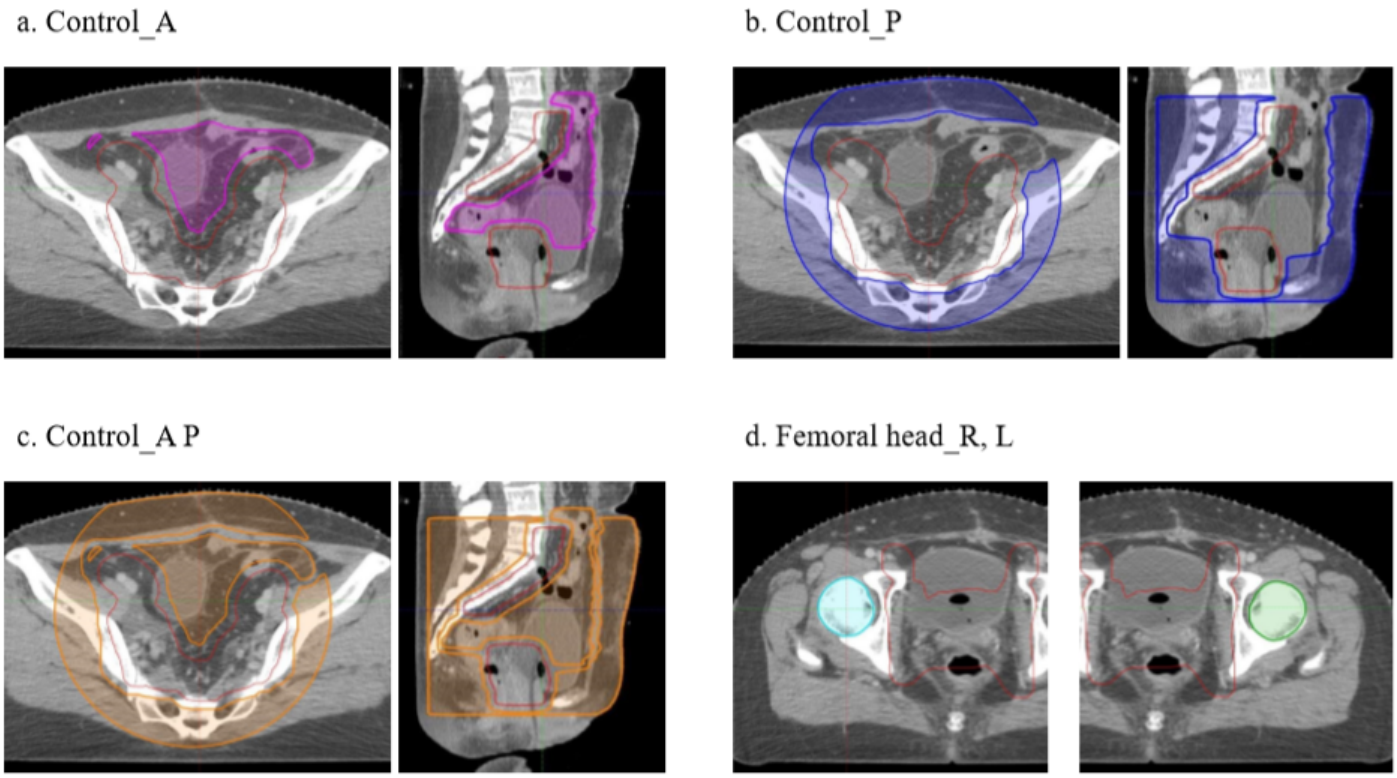

Figure 1

Contouring of Control_A (a), Control_P (b), Control_A P (c), Femoral head_R and Femoral head_L (d). Red contours represent the planning target volume.

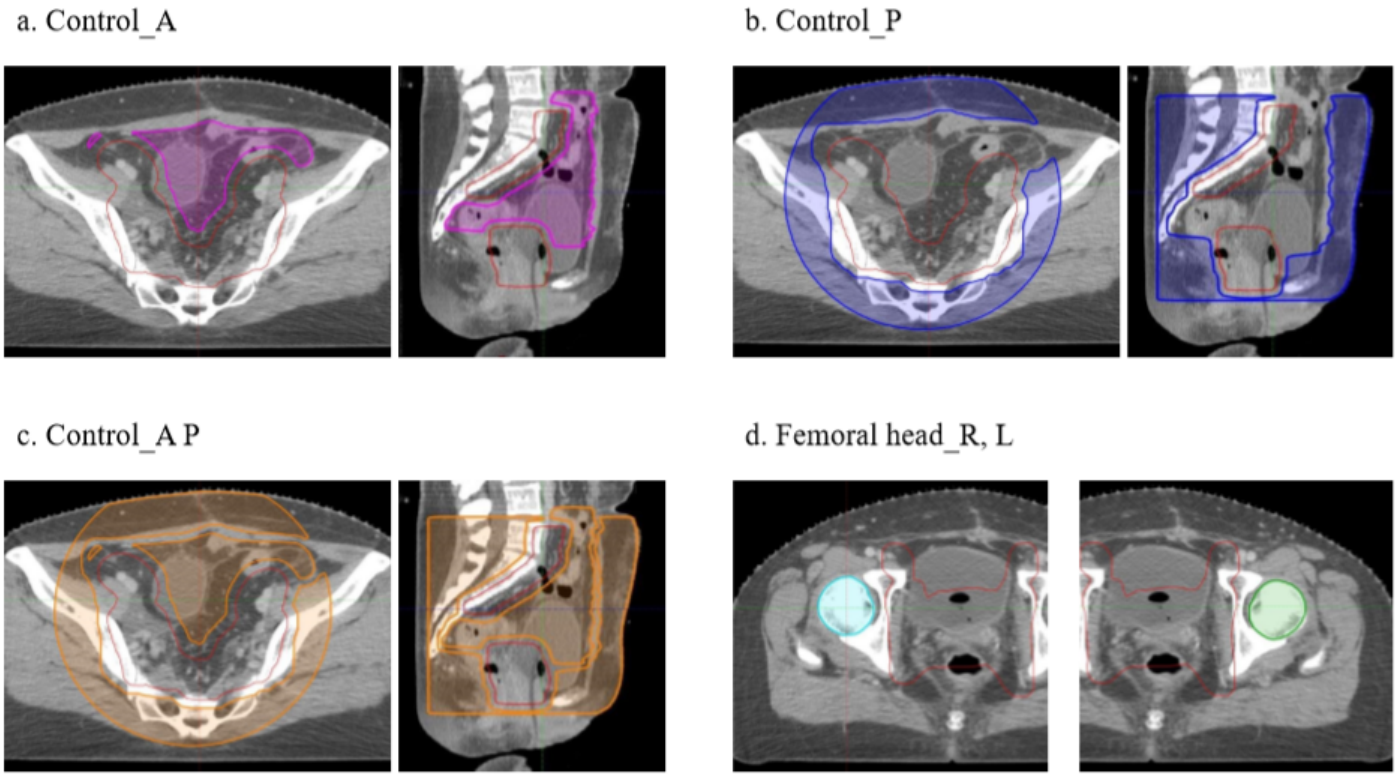

Figure 1

Contouring of Control_A (a), Control_P (b), Control_A P (c), Femoral head_R and Femoral head_L (d). Red contours represent the planning target volume.

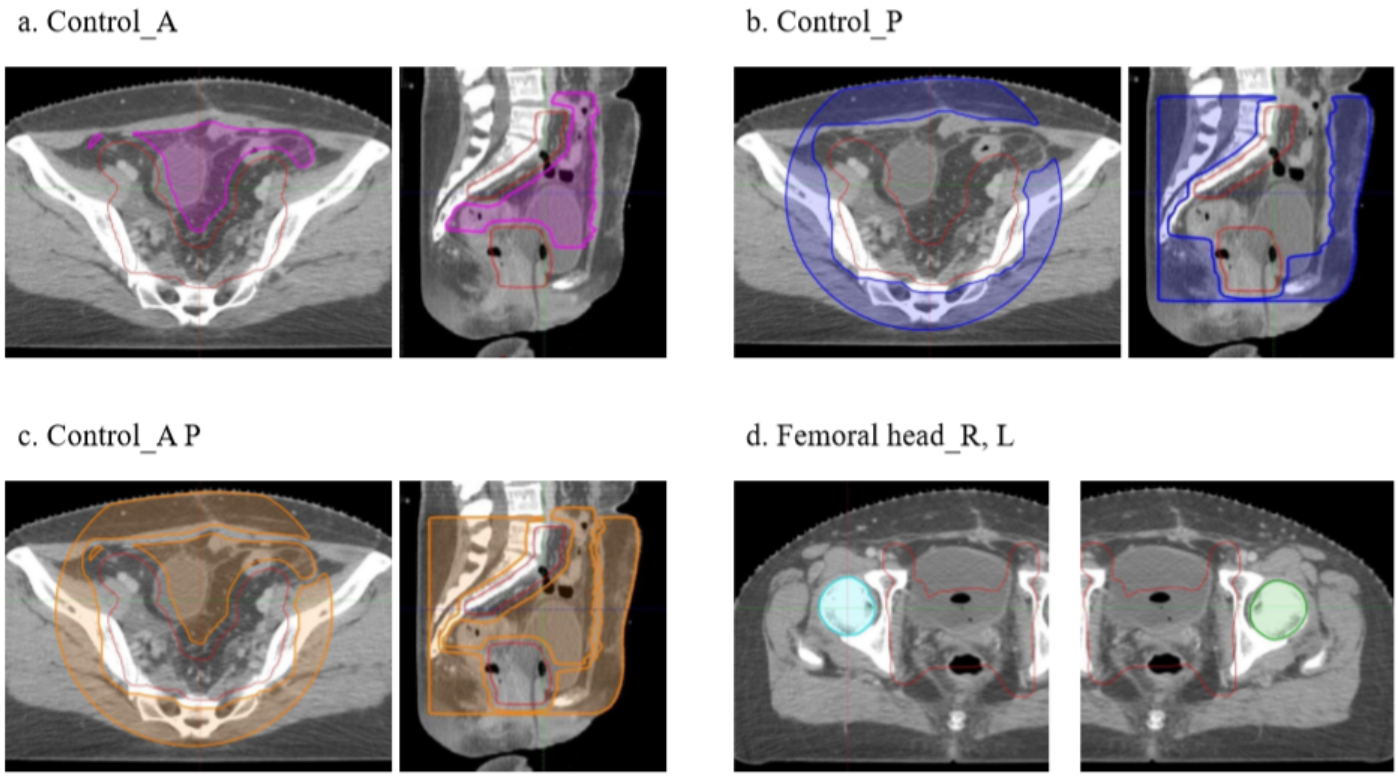

Figure 1

Contouring of Control_A (a), Control_P (b), Control_A P (c), Femoral head_R and Femoral head_L (d). Red contours represent the planning target volume.

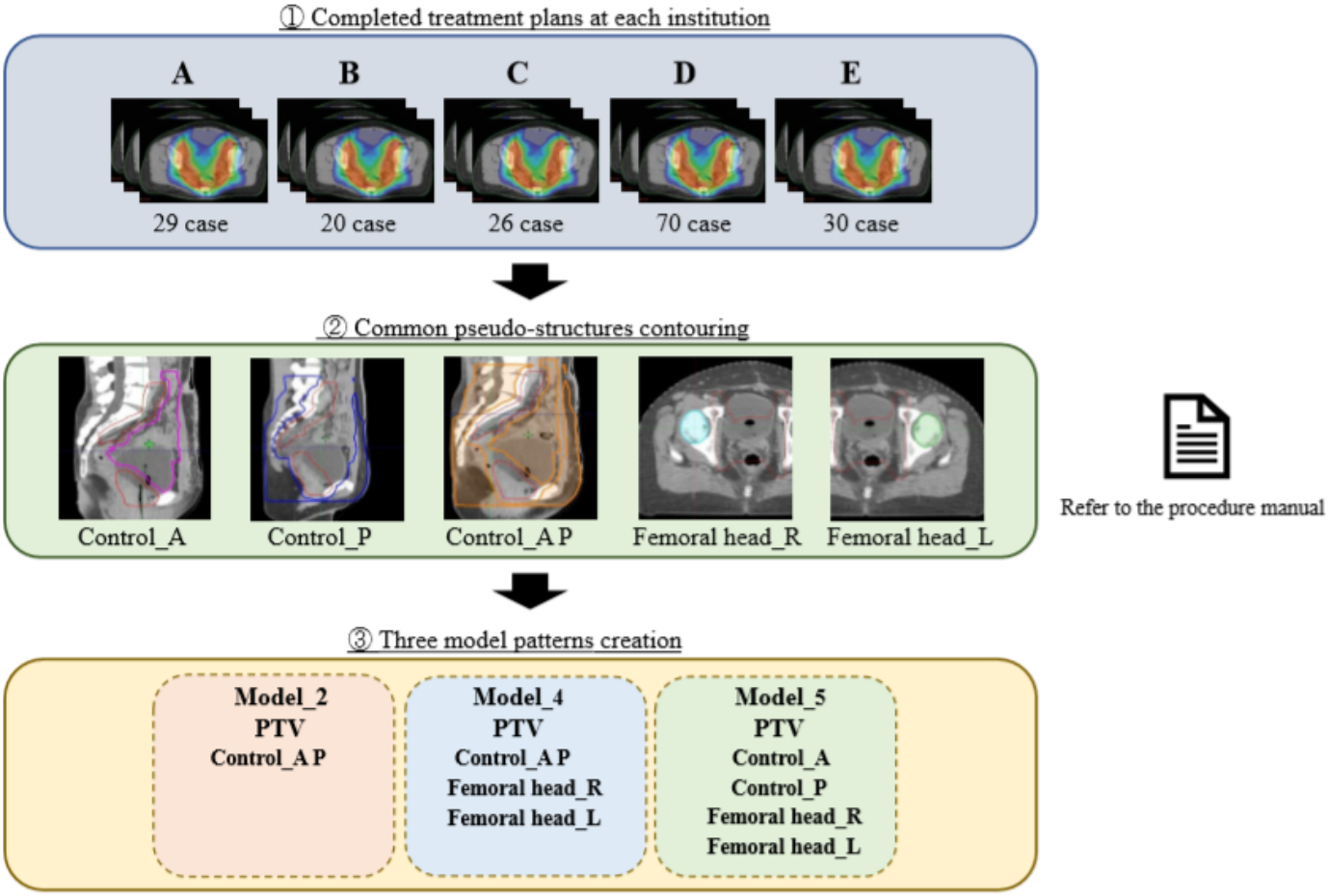

Figure 2

The process of contouring pseudo-structures and configuring the three model patterns. Letters A to E represent the different institutions.

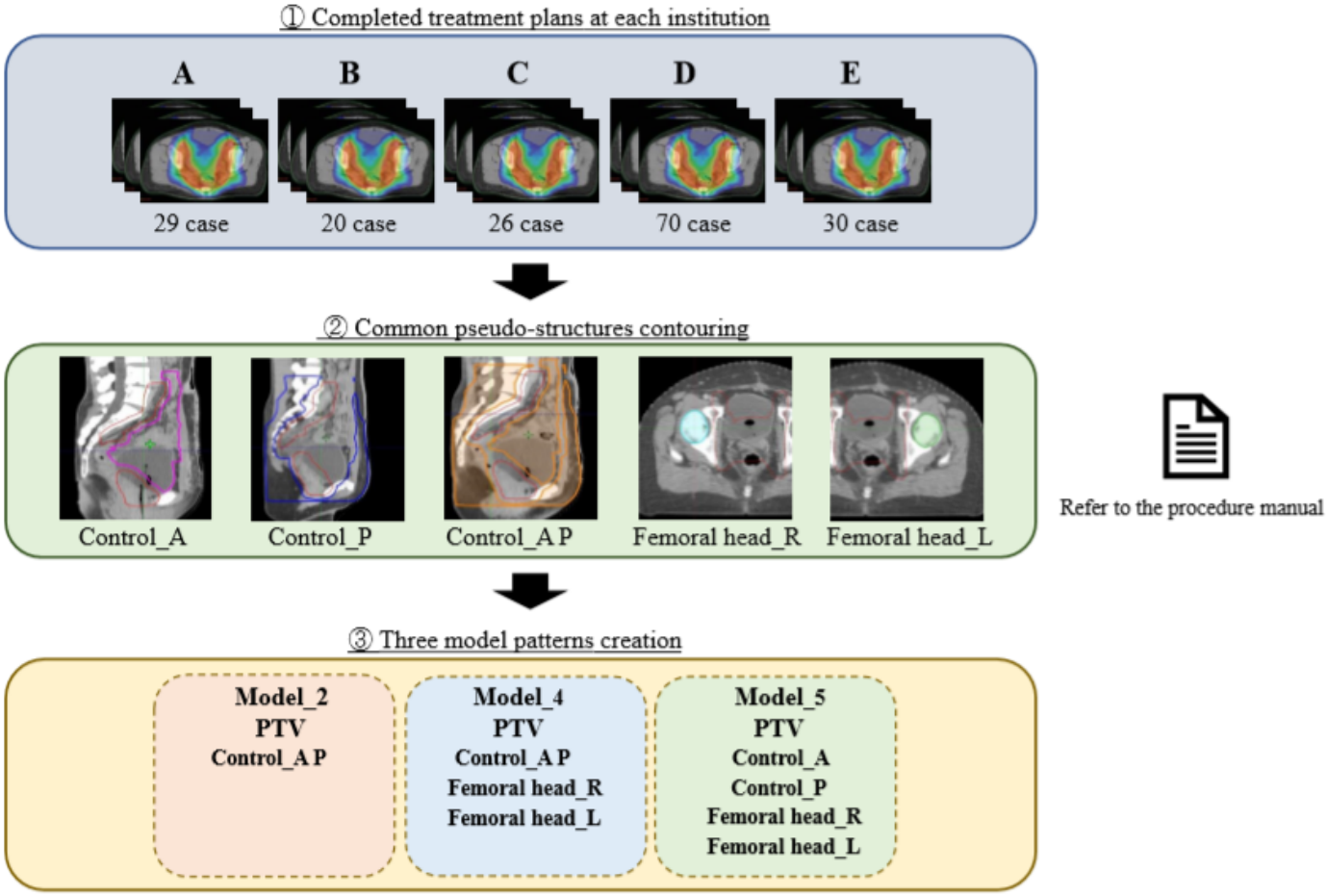

Figure 2

The process of contouring pseudo-structures and configuring the three model patterns. Letters A to E represent the different institutions.

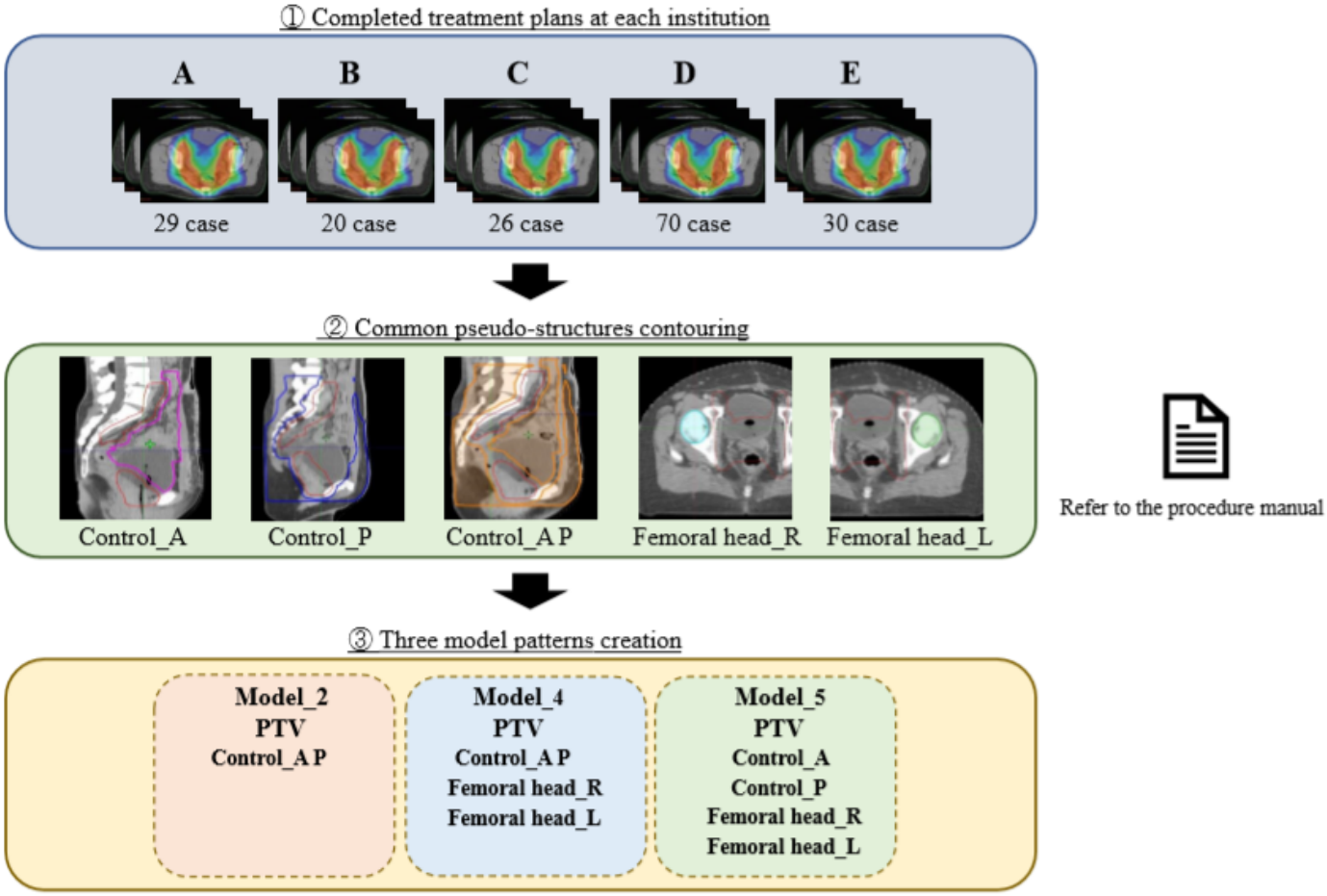

Figure 2

The process of contouring pseudo-structures and configuring the three model patterns. Letters A to E represent the different institutions.

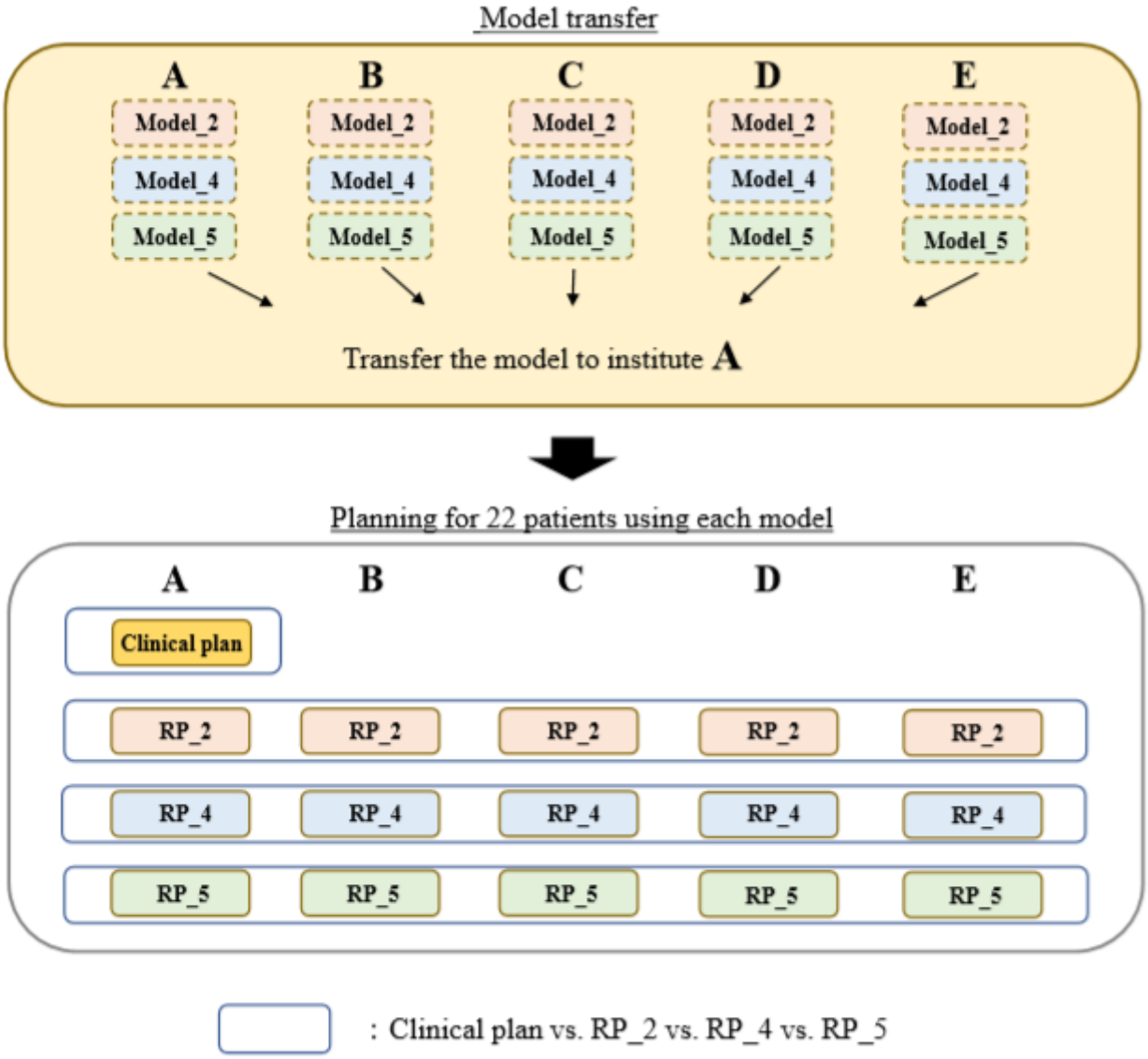

Figure 3

The process for the model transfer and plan comparison. Letters A to E represent the different institutions.

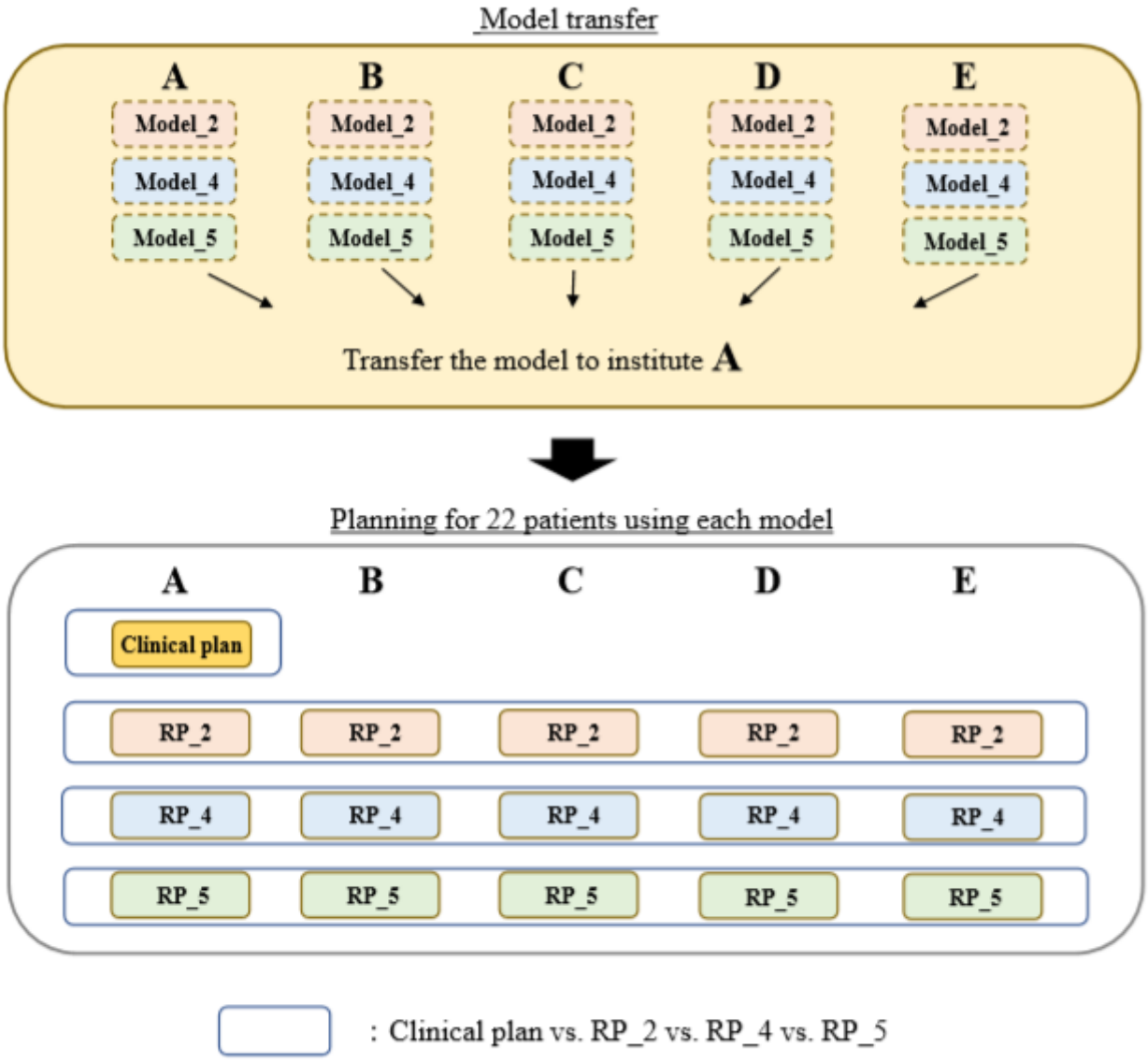

Figure 3

The process for the model transfer and plan comparison. Letters A to E represent the different institutions.

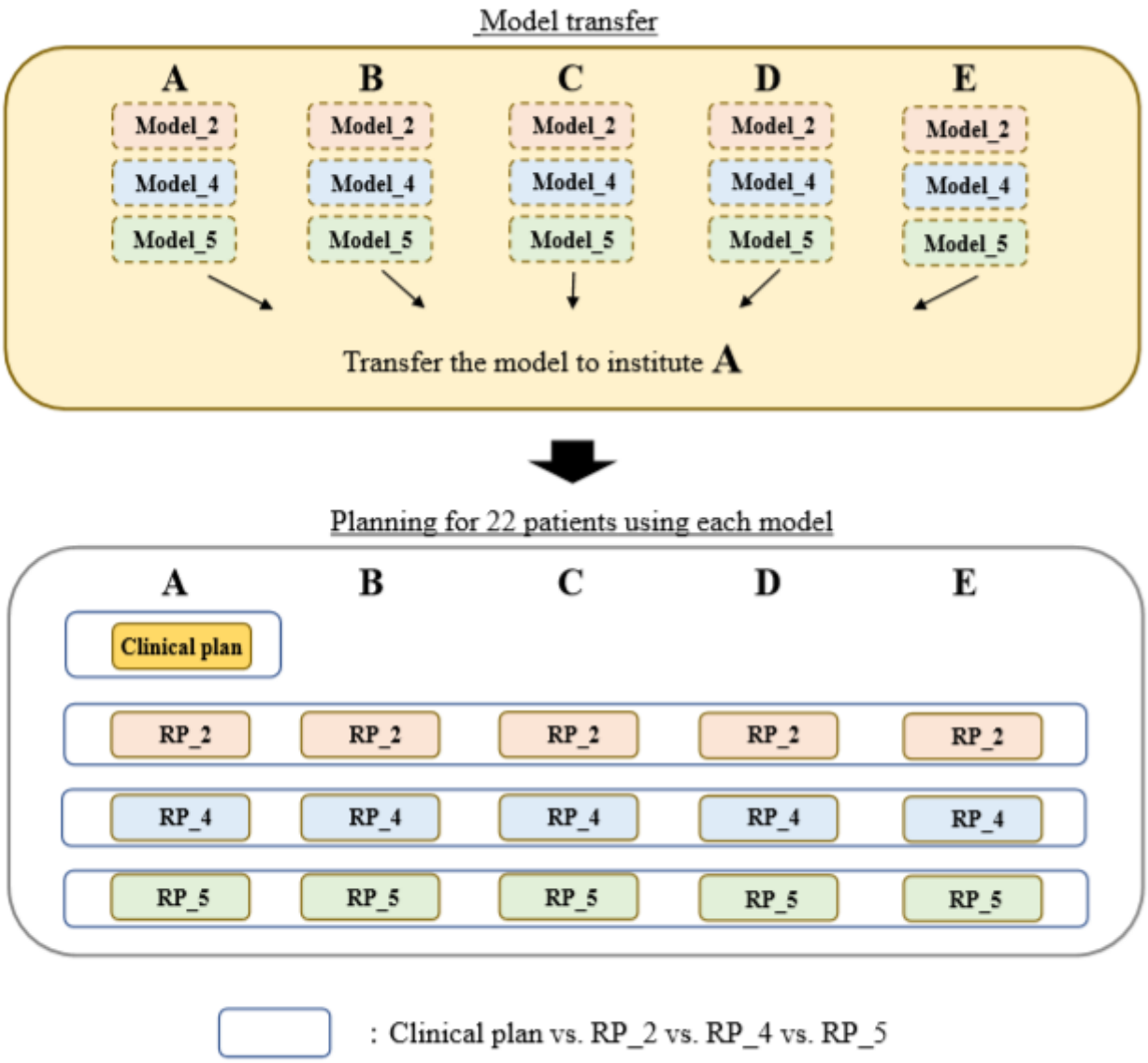

Figure 3

The process for the model transfer and plan comparison. Letters A to E represent the different institutions.

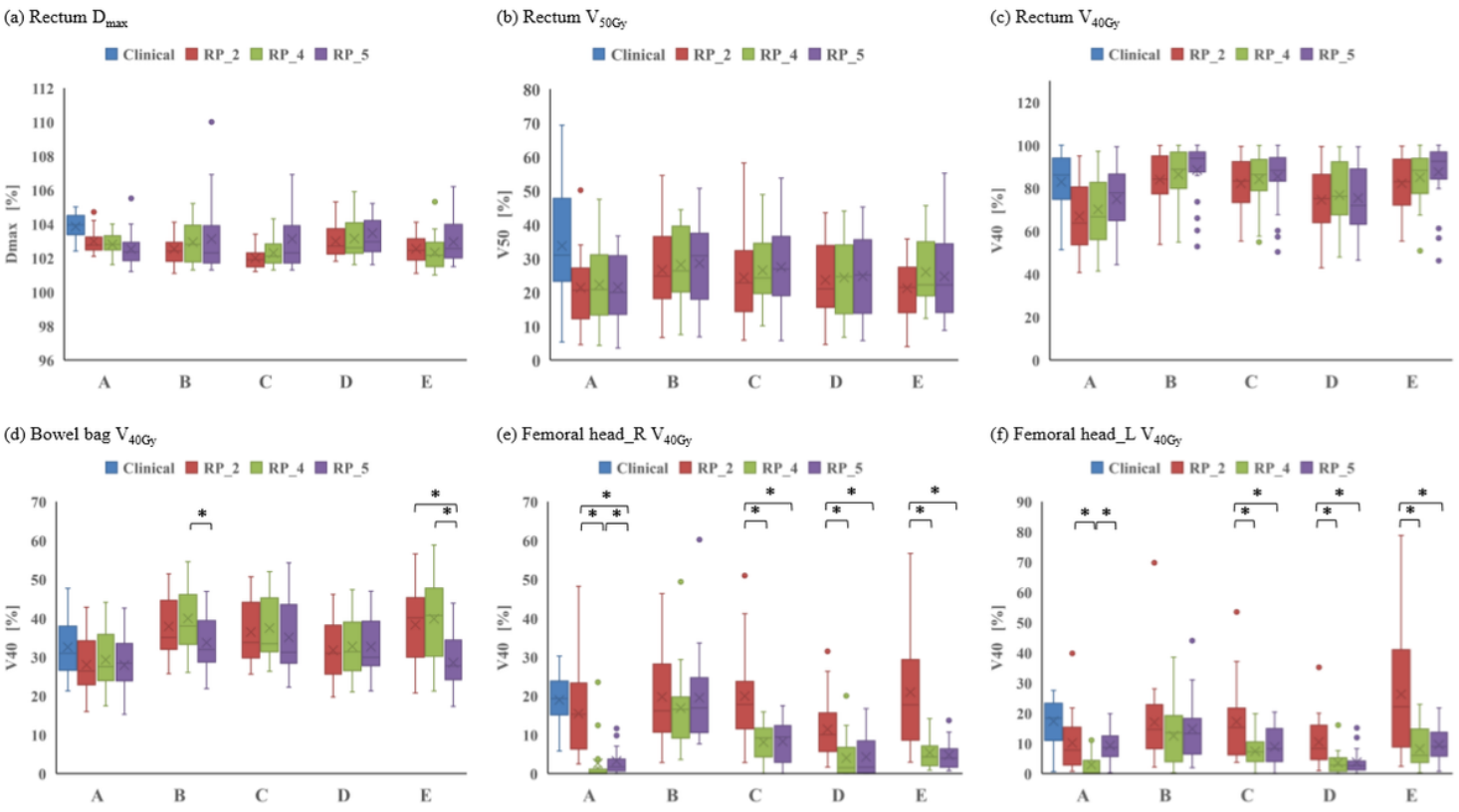

Figure 4

Box-and-whisker plots showing Rectum Dmax (a), Rectum V50Gy (b), Rectum V40Gy (c), Bowel bag V40Gy (d), Femoral head_R V40Gy (e), Femoral head_L V40Gy (f). The upper and lower edges represent the 25th (Q1) and 75th (Q3) percentiles, respectively. Whiskers represent the standard deviation. Outliers are marked with circles and were defined according to 1.5× the interquartile range. *, $p < 0.05$. Letters A to E represent the different institutions.

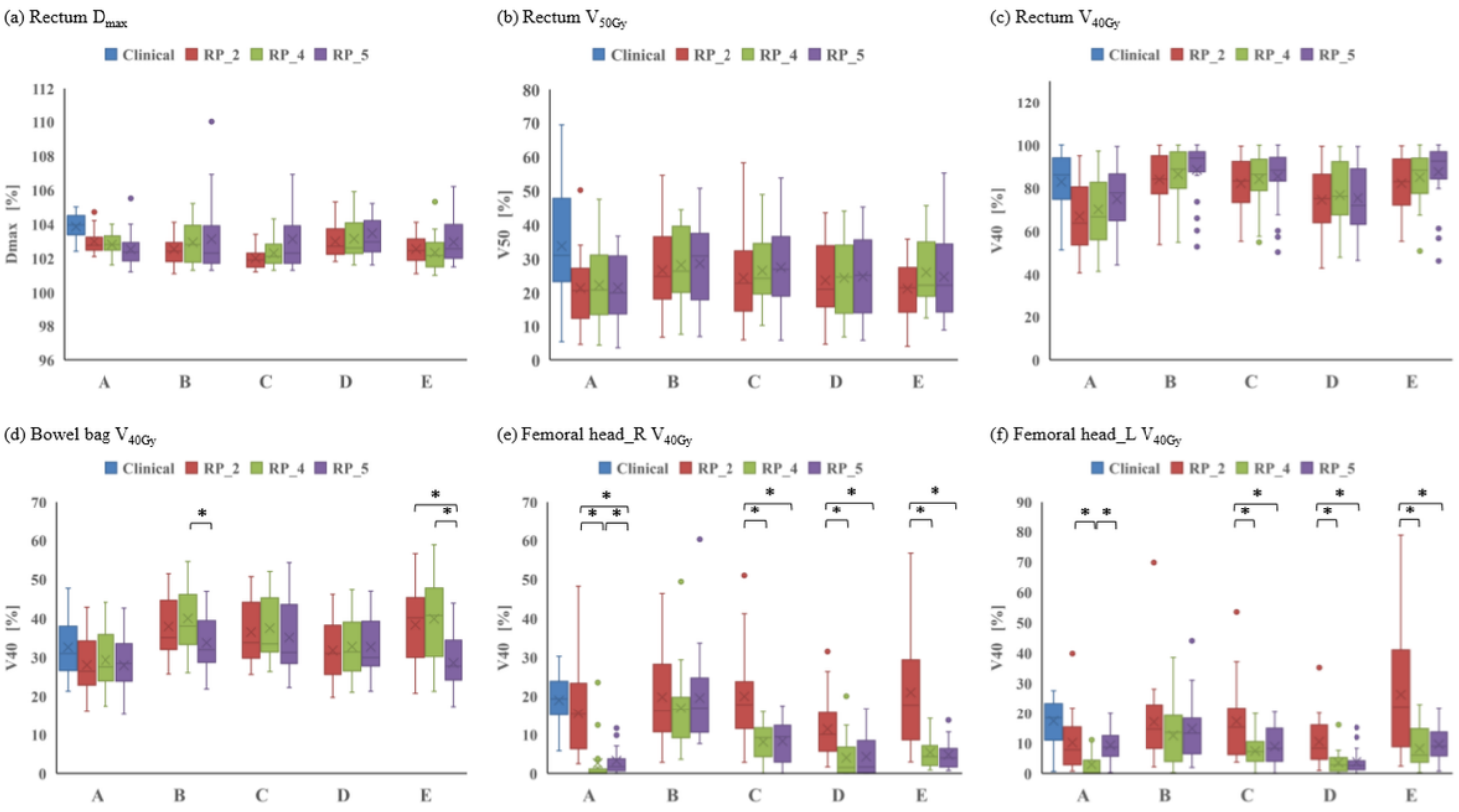

Figure 4

Box-and-whisker plots showing Rectum Dmax (a), Rectum V50Gy (b), Rectum V40Gy (c), Bowel bag V40Gy (d), Femoral head_R V40Gy (e), Femoral head_L V40Gy (f). The upper and lower edges represent the 25th (Q1) and 75th (Q3) percentiles, respectively. Whiskers represent the standard deviation. Outliers are marked with circles and were defined according to 1.5× the interquartile range. *, $p < 0.05$. Letters A to E represent the different institutions.

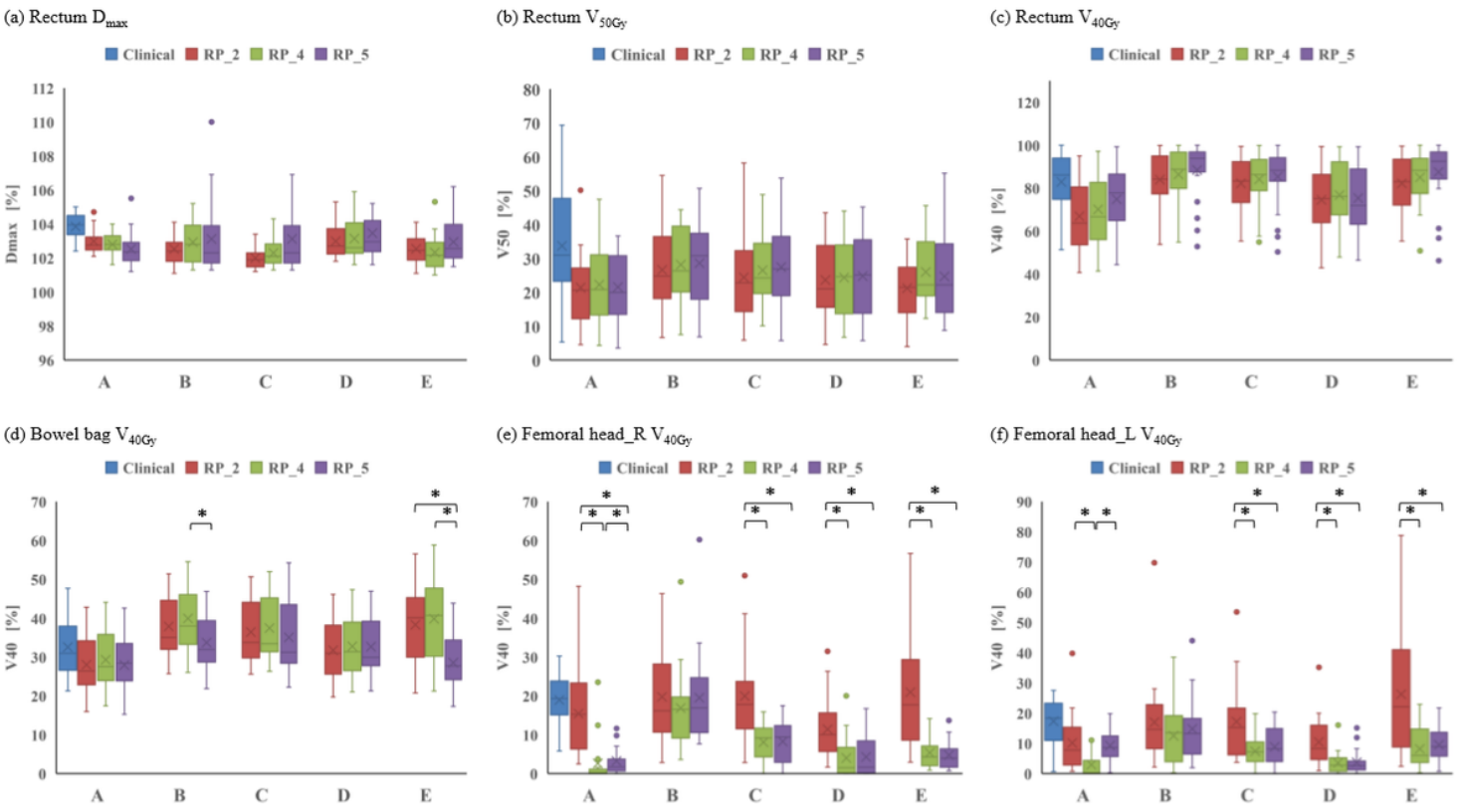

Figure 4

Box-and-whisker plots showing Rectum Dmax (a), Rectum V50Gy (b), Rectum V40Gy (c), Bowel bag V40Gy (d), Femoral head_R V40Gy (e), Femoral head_L V40Gy (f). The upper and lower edges represent the 25th (Q1) and 75th (Q3) percentiles, respectively. Whiskers represent the standard deviation. Outliers are marked with circles and were defined according to 1.5× the interquartile range. *, $p < 0.05$. Letters A to E represent the different institutions.